Liquid Crystals
Publication details, including instructions for authors and subscription information:
http://www.informaworld.com/smpp/title~content=t713926090

Methylene-linked liquid crystal dimers

Peter A. Henderson[a]; Olaf Niemeyer[a]; Corrie T. Imrie[a]
[a] Department of Chemistry, Meston Walk, University of Aberdeen, Old Aberdeen AB24 3UE, Scotland,

Online publication date: 06 August 2010

To cite this Article Henderson, Peter A. , Niemeyer, Olaf and Imrie, Corrie T.(2001) 'Methylene-linked liquid crystal dimers', Liquid Crystals, 28: 3, 463 — 472
To link to this Article: DOI: 10.1080/02678290010007558
URL: http://dx.doi.org/10.1080/02678290010007558

LIQUID CRYSTALS, 2001, VOL. 28, NO. 3, 463–472

Methylene-linked liquid crystal dimers

PETER A. HENDERSON, OLAF NIEMEYER and CORRIE T. IMRIE*

Department of Chemistry, Meston Walk, University of Aberdeen,
Old Aberdeen AB24 3UE, Scotland

(*Received 17 June 2000; accepted 21 August 2000*)

A range of symmetric liquid crystal dimers which differ in the nature of the link, either ether or methylene, between the spacer and mesogenic units has been prepared and their transitional properties characterized. The nematic–isotropic transition temperature, T_{NI}, and the associated entropy change, $\Delta S_{NI}/R$, are sensitive to the chemical nature of this link. Specifically, T_{NI} falls on replacing ether links with methylene links for both odd and even members although this reduction is more pronounced for odd members. In comparison, $\Delta S_{NI}/R$ increases on changing ether links for methylene links for even dimers, but decreases for odd-membered dimers. These observations are completely in accord with the predictions of a model developed by Luckhurst and co-workers in which the difference between the ether-linked and methylene-linked dimers rests exclusively in their shapes. Furthermore, the highly non-linear pentamethylene-linked dimers show a greater tendency to exhibit smectic behaviour; this is interpreted in terms of molecular packing giving rise to an alternating smectic phase.

1. Introduction

Liquid crystal dimers consist of molecules containing two mesogenic units separated by a flexible spacer, most commonly an alkylene chain [1–3]. One of the main characteristics of this class of materials is the pronounced alternation of the transitional properties on varying the number of methylene groups in the spacer. For example, both the nematic–isotropic transition temperature, T_{NI}, and the associated entropy change, $\Delta S_{NI}/R$, depend critically on the length and parity of the spacer. The alternation in T_{NI} is attenuated as the length of the spacer is increased, unlike that exhibited by $\Delta S_{NI}/R$ which remains essentially unaffected. These characteristic differences in behaviour between odd- and even-membered dimers are most often attributed to the dependence of the molecular shape on the parity of the spacer when considered in the all-*trans*-conformation. Thus, in an even-membered dimer the mesogenic groups are antiparallel, whereas in an odd-membered dimer they are inclined. The more linear structure of the even-membered dimers is then considered to be more compatible with the molecular organization found in the nematic phase resulting in, for example, higher values of $\Delta S_{NI}/R$ than found for odd-members. Such an argument clearly neglects the flexibility of the spacer and a more realistic interpretation of the transitional behaviour of dimers considers a range of conformations of the spacer and not solely the all-*trans*-conformation [1].

* Author for correspondence; e-mail: c.t.imrie@abdn.ac.uk

The magnitudes of these odd–even effects exhibited by T_{NI} and $\Delta S_{NI}/R$ on varying the number of groups in the spacer are strongly dependent on the nature of the group linking the spacer to the mesogenic cores. This is best illustrated by comparing the transitional properties of the α,ω-bis(4-cyanobiphenyl-4′-yloxy)alkanes [4],

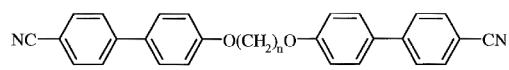

with those of the α,ω-bis(4-cyanobiphenyl-4′-yl)alkanes [3, 5].

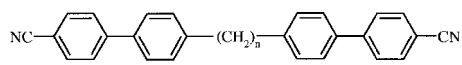

It should be noted that to make meaningful comparisons between these series we must compare members having the same number of atoms connecting the two mesogenic units. The nematic–isotropic transition temperatures are higher for the ether- than for the methylene-linked dimers and this difference is greater for odd members of the series. Thus, the magnitude of the alternation in T_{NI} exhibited by the methylene-linked series is larger than that seen for the ether-linked series. The alternation in $\Delta S_{NI}/R$ is also more pronounced for the methylene-linked series, although the even members of this series now exhibit higher values of $\Delta S_{NI}/R$ than the corresponding ether-linked dimers, while this is reversed for the odd members.

Luckhurst and his co-workers have suggested that the differences in the transitional behaviour of ether- and methylene-linked dimers arise from differences in

Liquid Crystals ISSN 0267-8292 print/ISSN 1366-5855 online © 2001 Taylor & Francis Ltd
http://www.tandf.co.uk/journals
DOI: 10.1080/02678290010007558

molecular geometry and, specifically, from the bond angle between the *para*-axis of the mesogen and the first bond in the spacer [6, 7]. For the methylene-linked dimers this bond angle is 113.5° while for ether-linked dimers it is 126.4°. This difference effects the molecular shape such that the all-*trans*-conformation of an ether-linked dimer is now more linear than the corresponding methylene-linked material, see figure 1. The greater shape anisotropy of the ether-linked materials would be expected to give rise to higher nematic–isotropic transition temperatures. This view was supported by calculated T_{NI} values for the two series obtained using a molecular field theory [8] in which the only difference between the calculations for the two series was this bond angle [6]. The predictions of this theory were in good agreement with the experimental data, and furthermore it was shown that geometrical factors alone could also account for the differences in $\Delta S_{NI}/R$ for the ether- and methylene-linked dimers [7].

In a more transparent model developed by Luckhurst and co-workers, to understand how geometrical factors influence the transitional properties of dimers, the dimers can adopt just two conformations, one linear and one bent [9, 10]. This approach makes the intriguing prediction that systems containing high concentrations of bent conformers in the isotropic phase, i.e. dimers containing short odd-membered methylene-linked spacers, should exhibit a nematic–nematic transition [9, 10]. The nematic–isotropic entropy exhibited by 1,5-bis(4-cyanobiphenyl-4′-yl)pentane is very small suggesting that the transition is approaching second order in nature [5]. Theory suggests that following such a second order transition a biaxial nematic phase should be observed. Unfortunately, this possibility could not be investigated for this particular dimer as experimentally it exhibited a smectic phase obscuring any possible nematic–nematic transition.

It appears, therefore, that the transitional properties of dimers can be accounted for successfully solely in terms of geometrical factors. These models have been tested, however, for just one set of materials; hence, here we describe the transitional behaviour of a range of methylene-linked dimers and compare them with the analogous ether-linked materials. Furthermore, this provides an opportunity to explore the exciting possibility that highly bent dimers will exhibit a nematic–nematic transition. The range of dimers investigated, and the acronyms used to describe them, are shown in figure 2. In each acronym *n* refers to the number of carbon atoms in the central spacer. For comparative purposes we consider dimers containing the same number of atoms linking the two mesogenic groups. Thus the properties of *X*-5-*X* are compared with those of *X*-O3O-*X* while *X*-6-*X* is compared with *X*-O4O-*X*. *m* refers to the number of carbon atoms in the terminal chain and in all these cases $m = 1$ or 2.

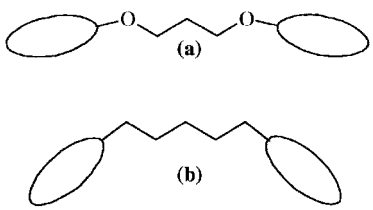

Figure 1. Schematic representations of the molecular shape of the all-*trans*-conformation of an odd-membered dimer containing (*a*) an ether and (*b*) a methylene-linked spacer.

2. Experimental

The synthesis of each group of dimers involved two steps: first the synthesis of either the methylene- or ether-linked diaminophenyl-based central unit, see schemes 1 and 2, respectively; then the subsequent reaction of these with the appropriate functionalized benzaldehyde, see scheme 3. The synthetic methods for the homologues of each series were identical and hence only representative syntheses for each series are given.

2.1. *Materials*

All chemicals were used as received (Aldrich) except for the *n*-alkyl- and *n*-alkoxy-benzaldehydes and acetyl

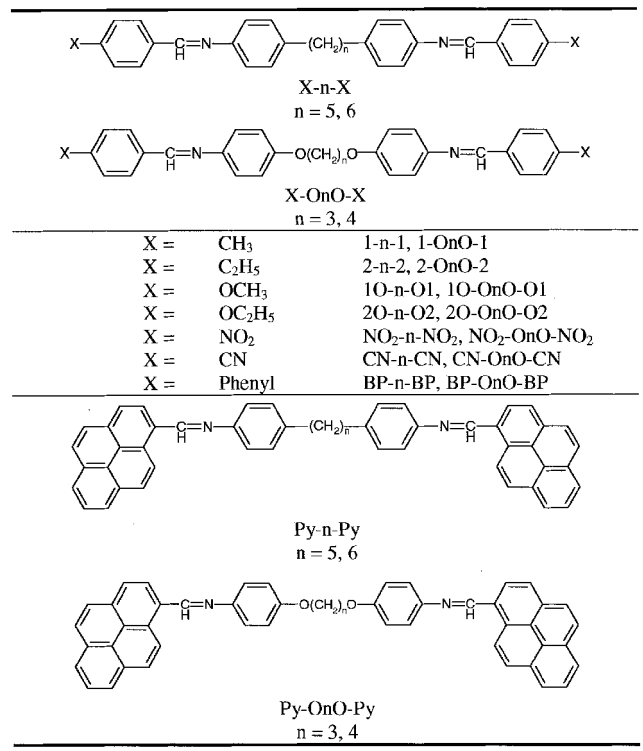

Figure 2. Structures showing a range of methylene- and ether-linked dimers and their acronyms.

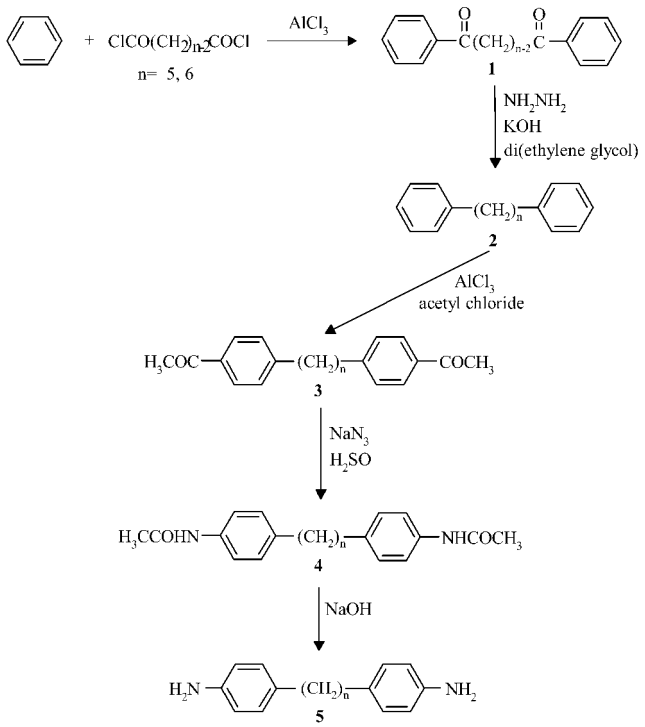

Scheme 1.

chloride which were redistilled immediately prior to use. Benzene was dried over calcium hydride.

2.2. *Characterization*

All the dimers and their intermediates were characterized using a combination of ^{1}H NMR, using a Bruker AC-F 250 MHz spectrometer, FTIR spectroscopy using an ATI Mattson Genesis Series FTIR spectrometer, and elemental analysis carried out by Butterworth Laboratories.

2.3. *Synthesis of 1,5-bis(4-aminophenyl-1-)pentane , **5** (n = 5)*

The synthesis of 1,5-bis(4-aminophenyl-1-)pentane, **5** ($n = 5$), is shown in scheme 1; this is a modification of the synthetic route described by Keller and Liebert [11] for the preparation of 4-alkylanilines.

2.3.1. *1,5-Diphenylpentane-1,5-dione, **1***

Compound **1** was prepared using Freidel–Crafts acetylation. A stirred suspension of powdered anhydrous aluminium chloride (66.6 g, 0.5 mol) in dry benzene (350 ml) was cooled in an ice bath and glutaryl dichloride (27 ml, 0.21 mol) was added dropwise over a period of 30 min. The reaction mixture was allowed to warm to room temperature and stirred for a further 2 h. It was

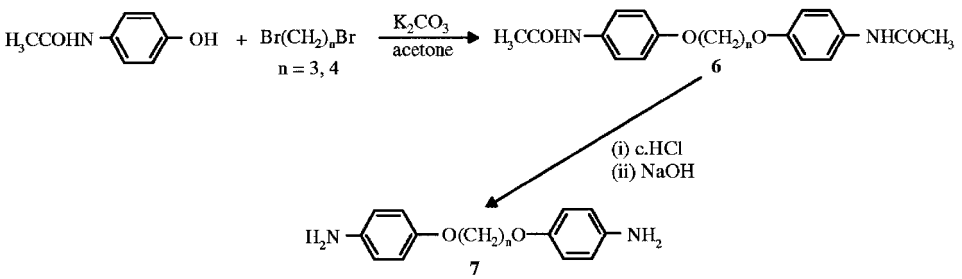

Scheme 2.

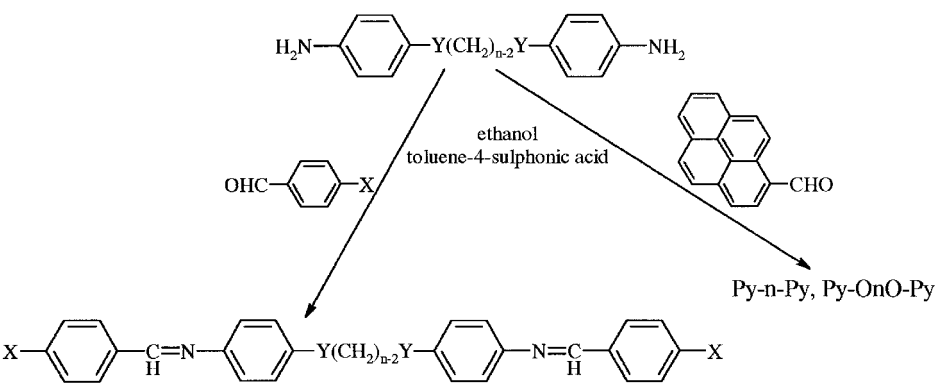

n = 5, 6, X = CH_3, C_2H_5, CH_3O, C_2H_5O, phenyl, CN, NO_2, Y = O, CH_2

Scheme 3.

then poured into a mixture of ice (350 g) and concentrated hydrochloric acid (67 ml) and the organic layer was separated and washed with 5% sodium hydroxide solution and then water. The benzene was removed by rotary evaporation and the resulting white solid recrystallized from ethanol; yield 21.8 g, 41%, m.p. 68°C. ^{1}H NMR ($CDCl_3$) δ (ppm): 8.0 (m, 4H, Ar–H), 7.5–7.4 (m, 6H, Ar–H), 3.1 (t, 4H, $COC\underline{H}_2CH_2$, J = 6.9 Hz), 2.2 (qn, 2H, $CH_2C\underline{H}_2CH_2$, J = 7 Hz). IR (KBr) ν (cm^{-1}): 1679 (CO); 731 (monosubstituted aromatic).

2.3.2. *1,5-Diphenylpentane,* ***2***

Compound **2** was prepared using a modified Huang–Minlon reduction. A mixture containing **1** (25 g, 0.1 mol), diethylene diglycol (180 ml), 98% hydrazine monohydrate (17.3 ml, 0.357 mol) and potassium hydroxide (23.6 g, 0.42 mol) was heated at 140°C for 4.5 h. The reaction mixture was cooled and the product extracted five times using diethyl ether (100 ml portions). The combined organic layers were dried over anhydrous magnesium sulphate and the solvent removed by rotary evaporation. The residue was distilled on a Kugelrohr apparatus at 140°C/6.5 mm Hg, yielding an orange liquid. The IR spectrum of the product did not contain the band associated with the carbonyl group in the spectrum of **1**; yield 13.0 g, 58.5%. ^{1}H NMR ($CDCl_3$) δ (ppm): 7.4–7.1 (m, 10H, Ar–H) 2.7 (t, 4H, ArC$\underline{H}$2CH2, J = 7.8 Hz), 1.7 (qn, 4H, $CH_2C\underline{H}_2CH_2C\underline{H}_2CH_2$, J = 7.8 Hz), 1.5 (m, 2H, $CH_2CH_2C\underline{H}_2CH_2CH_2$). IR (KBr) ν (cm^{-1}): 3025, 1602, 1495 (Ar–H), 2926, 2854, 1454 (CH_2); 746, 687 (monosubstituted aromatic).

2.3.3. *1,5-Bis(4-acetophenyl-1-)pentane,* ***3*** [7]

Compound **2** (13 g, 59 mmol) was added dropwise to a stirred mixture of freshly ground aluminium chloride (23.6 g, 0.18 mol) and acetyl chloride (8.86 g, 0.12 mol) in absolute chloroform (150 ml), cooled to 0°C in an ice/water bath. The ice bath was removed and the mixture allowed to warm to room temperature and stirred for a further 2 h. The reaction mixture was poured into a well stirred solution of concentrated hydrochloric acid (70 ml) and ice (150 g). The organic layer was collected and washed twice with concentrated hydrochloric acid (50 ml), once with sodium hydrogen carbonate solution (100 ml) and finally with water (100 ml). The solvent was removed by rotary evaporation to yield a brown liquid, which was used without further purification; yield 16.0 g, 87.8%. ^{1}H NMR ($CDCl_3$) δ (ppm): 7.9 (d, 4H, Ar–H, J = 8.25 Hz), 7.2 (d, 4H, Ar–H, J = 8 Hz), 2.65 (t, 4H, $ArC\underline{H}_2CH_2$, J = 7.6 Hz), 2.58 (s, 6H, $ArCOC\underline{H}_3$), 1.7 (qn, 4H, $CH_2C\underline{H}_2CH_2C\underline{H}_2CH_2$, J = 7.6 Hz), 1.4 (m, 2H, $CH_2CH_2C\underline{H}_2CH_2CH_2$). IR (KBr) ν (cm^{-1}): 3003, 1606, 1570 (Ar–H); 2933, 2857, 1412, 1358, 957 (CH_2) 1684 (aryl C=O).

2.3.4. *1,5-Bis(4-acetamidophenyl-1-)pentane,* ***4***

A mixture containing **3** (15 g, 0.048 mol), dichloromethane (50 ml) and 70% sulphuric acid (140 ml) was stirred in a chilled water bath. Sodium azide (6.77 g, 0.106 mol) was added slowly. Specifically, about a 10% portion was added initially and, after nitrogen began to evolve, the remainder was added slowly in small portions and the temperature maintained between 15 and 20°C. The reaction mixture was stirred overnight and poured into a mixture of chilled water (200 ml) and dichloromethane (110 ml). The organic layer was separated and washed with sodium hydrogen carbonate solution (50 ml) and water (50 ml). The aqueous layers were combined and shaken with dichloromethane. The organic layers were combined and reduced to *c.* 10 ml, and 60–80° petroleum spirit (150 ml) was added. The resulting white precipitate was collected and recrystallized from ethanol; yield 6.7 g, 41.2%, m.p. 177–178°C. ^{1}H NMR ($CDCl_3$) δ (ppm): 7.3 (m, 4H, Ar–H), 7.2 (s, 2H, CON$\underline{H}$Ar), 7.1 (m, 4H, Ar–H), 2.6 (t, 4H, $ArC\underline{H}_2CH_2$, J = 7.5 Hz), 2.1 (s, 6H, $C\underline{H}_3CO$), 1.6 (qn, 4H, $CH_2C\underline{H}_2CH_2C\underline{H}_2CH_2$, J = 7.5 Hz), 1.3 (m, 2H, $CH_2CH_2C\underline{H}_2CH_2CH_2$). IR (KBr) ν (cm^{-1}): 3293, 3187, 1657 (CONH), 1371 (CH_3), 837 (*p*-substituted aromatic).

2.3.5. *1,5-Bis(4-aminophenyl-1-)pentane,* ***5****, (n = 5)*

A mixture containing **4** (5.6 g, 0.017 mol), ethanol (50 ml) and sodium hydroxide (31.3 g dissolved in 30 ml water) was heated at reflux overnight. The mixture was cooled, concentrated by rotary evaporation, poured into ice/water (100 ml) and the resulting pale brown precipitate recrystallized from ethanol; yield 2.5 g, 56.6%, m.p. 103–104°C. ^{1}H NMR ($CDCl_3$) δ (ppm): 6.9 (d, 4H, Ar–H, J = 8 Hz), 6.6 (d, 4H, Ar–H, J = 8.4 Hz), 3.4 (s, 4H, $ArN\underline{H}_2$), 2.5 (t, 4H, $ArC\underline{H}_2CH_2$, J = 7.8 Hz), 1.6 (qn, 4H, $CH_2C\underline{H}_2CH_2C\underline{H}_2CH_2$, J = 7.7 Hz), 1.4 (m, 2H, $CH_2CH_2C\underline{H}_2CH_2CH_2$). IR (KBr) ν (cm^{-1}): 3426, 3342, 1625 (NH_2), 3010, 1515, 821 (*p*-substituted aromatic), 1465, 751 (CH_2).

2.4. *Synthesis of 1,6-bis(4-aminophenyl-1-)hexane ,* ***5*** *(n = 6)*

1,6-Bis(4-aminophenyl-1-)hexane, was synthesized in a similar manner to compound **5** (n = 5), and the spectroscopic data for it and its intermediates are given.

2.4.1. *1,6-Diphenylhexane-1,6-dione*

M.p. 110–112°C. ^{1}H NMR ($CDCl_3$) δ (ppm): 7.9 (m, 4H, Ar–H), 7.6–7.4 (m, 6H, Ar–H), 3.0 (t, 4H, $COC\underline{H}_2CH_2$, J = 7.0 Hz), 1.8 (qn, 4H, $CH_2C\underline{H}_2C\underline{H}_2CH_2$, J = 3.4 Hz). IR (KBr) ν (cm^{-1}): 2933, 2855 (CH_2), 1679 (ArCO), 1603, 731 (monosubstituted aromatic).

2.4.2. *1,6-Diphenylhexane*

^{1}H NMR ($CDCl_3$) δ (ppm): 7.4–7.2 (m, 10H, Ar–H), 2.6, (t, 4H, $ArC\underline{H}_2CH_2$, J = 7.6 Hz), 1.6 (m, 4H, $CH_2C\underline{H}_2CH_2CH_2C\underline{H}_2CH_2$), 1.4 (qn, 4H, CH_2CH_2-$C\underline{H}_2C\underline{H}_2CH_2CH_2$, J = 3.8 Hz). IR (KBr) ν (cm^{-1}): 3025, 1603, 1495, 746, 698 (monosubstituted aromatic), 2929, 2854, 1453, 905 (CH_2).

2.4.3. *1,6-Bis(4-acetophenyl-1-hexane*

After solvent extraction this product was obtained as a white powder, and recrystallized from ethanol. M.p. 105–107°C. ^{1}H NMR ($CDCl_3$) δ (ppm): 7.8 (d, 4H, Ar–H, J = 8.3 Hz), 7.2 (d, 4H, Ar–H, J = 7.8 Hz), 2.65 (t, 4H, $ArC\underline{H}_2CH_2$, J = 7.6 Hz), 2.58 (s, 6H, $ArCOC\underline{H}_3$), 1.6 (m, 4H, $C\underline{H}_2$), 1.3 (m, 4H, $C\underline{H}_2$). IR (KBr) ν (cm^{-1}): 1604, 814 (*p*-substituted aromatic), 2934, 2854, 1465 (CH_2), 1679 (aryl C=O), 1362 ($COCH_3$).

2.4.4. *1,6-Bis(4-acetamidophenyl-1-)hexane*

M.p. 221–222°C. ^{1}H NMR ($CDCl_3$) δ (ppm): 9.8 (s, 2H, $CON\underline{H}Ar$), 7.4 (d, 4H, Ar–H, J = 8.5 Hz), 7.1 (d, 4H, Ar–H, J = 8.5 Hz), 2.5 (t, 4H, $ArC\underline{H}_2CH_2$, J = 7.4 Hz), 2.0 (s, 6H, $C\underline{H}_3CO$), 1.5 (m, 4H, $C\underline{H}_2$), 1.3 (m, 4H, $C\underline{H}_2$). IR (KBr) ν (cm^{-1}): 3310, 1666 (CONH), 2928, 2852 (CH_2, CH_3), 1604, 1516, 838 (*p*-substituted aromatic).

2.4.5. *1,6-Bis(4-aminophenyl-1-)hexane,* **5** *(n = 6)*

M.p. 122–123°C. ^{1}H NMR ($CDCl_3$) δ (ppm): 6.9 (d, 4H, Ar–H, J = 8.3 Hz), 6.6 (d, 4H, Ar–H, J = 8.2 Hz), 3.5 (s, 4H, $ArN\underline{H}_2$), 2.5 (t, 4H, $ArC\underline{H}_2CH_2$, J = 7.6 Hz), 1.6 (m, 4H, $C\underline{H}_2$), 1.3 (m, 4H, $C\underline{H}_2$). IR (KBr) ν (cm^{-1}): 3422, 3346, 1629 (NH_2); 3014, 1516, 825 (*p*-substituted aromatic); 2913, 2850, 1465 (CH_2).

2.5. *Synthesis of 1,3-bis(4-aminophenyl-1-oxy)propane,* **7**, *(n = 3)*

1,3-Bis(4-aminophenyl-1-oxy)propane, (**7** in scheme 2), was prepared using the synthetic route shown in scheme 2. 1,4-Bis(4-acetamidophenyl-1-oxy)butane (**7**, n = 4) was prepared using the same method. It was hydrolysed using the method described in §2.3.5, except that potassium hydroxide was used in place of sodium hydroxide.

2.5.1. *1,3-Bis(4-acetamidophenyl-1-oxy)propane,* ***6***

A mixture containing 1,3-dibromopropane (17.7 g, 0.088 mol), 4-acetamidophenol (27.8 g, 0.184 mol), potassium carbonate (60.5 g, 0.44 mol) and acetone (250 ml) was heated at reflux with stirring overnight. The mixture was cooled and poured into water (2.5 l). The resulting white precipitate was collected and recrystallized from ethanol. No NMR could be obtained due to the insolubility of the product; yield 14.5 g, 48.2%, m.p. 191–192°C. IR (KBr): ν (cm^{-1}): 3315 (CONH), 1679 (CO).

2.5.2. *1,3-Bis(4-aminophenyl-1-oxy)propane, 7 (n = 3)*

A mixture containing **6** (13.8 g, 0.04 mol), ethanol (400 ml) and concentrated hydrochloric acid (100 ml) was heated at reflux with stirring overnight. The solution was cooled, poured over ice (500 g) and made alkaline with 50% NaOH solution. The precipitate was collected and recrystallized from toluene giving a pink solid; yield 7.3 g, 69.7%, m.p. 119–121°C. ^{1}H NMR ($CDCl_3$, δ): 6.7 (m, 4H, Ar–H), 6.6 (m, 4H, Ar–H), 4.1 (t, 4H, $OC\underline{H}_2CH_2$, J = 6.25 Hz), 3.3 (s, 4H, $ArN\underline{H}_2$), 2.1 (qn, 2H, $CH_2C\underline{H}_2CH_2$, J = 6.25 Hz). IR (KBr) ν (cm^{-1}): 3422, 3346, 1624 (NH_2 stretch), 3014, 1516, 825 (*p*-substituted aromatic), 1465 (CH_2), 1271 (C–O).

2.6. *Synthesis of 1,4-bis(4-aminophenyl-1-oxy)butane, 7 (n = 4)*

1,4-Bis(4-aminophenyl-1-oxy)butane was synthesized using the procedures described for **7** (n = 3), and spectroscopic data are given below.

2.6.1. *1,4-Bis(4-acetamidophenyl-1-oxy)butane*

M.p. 240–241°C. IR (KBr): ν (cm^{-1}): 3316, 3051, 1658 (CONH), 2957, 2873 (CH_2, CH_3), 1599, 1534, 829 (*p*-substituted aromatic) 1240 (ArCO).

2.6.2. *1,4-Bis(4-aminophenyl-1-oxy)butane, 7 (n = 4)*

M.p. 136–138°C. ^{1}H NMR ($CDCl_3$, δ): 6.8 (d, 4H, Ar–H, J = 8.8 Hz), 6.6 (d, 4H, Ar–H, J = 9 Hz), 3.9 (t, 4H, $OC\underline{H}_2CH_2$, J = 5.4 Hz), 3.4 (s, 4H, $ArN\underline{H}_2$), 1.9 (qn, 4H, $CH_2C\underline{H}_2C\underline{H}_2CH_2$, J = 2.75 Hz). IR (KBr) ν (cm^{-1}): 3391, 3311, 1637 (NH_2), 2924, 2865 (CH_2), 1591, 1510, 824 (*p*-substituted aromatic), 1382 (CH_3) 1232 (C–O).

2.7. *Synthesis of the dimer series (scheme 3)*

A representative method is described for 1O-5-O1. Thus, 4-methoxybenzaldehyde (1.3 mmol) was added to a stirred solution of 1,5-bis(4-aminophenyl-1-)pentane (0.15 g, 0.60 mmol) and a few crystals of toluene-4-sulphonic acid in hot ethanol. The reaction mixture was heated at reflux for 3 h. After cooling, the resulting precipitate was filtered off, washed with cold ethanol, and recrystallized twice from ethanol. All products were recrystallized from ethanol except for 1O-O3O-O1 and 2O-O3O-O2 which were recrystallized from chloroform, and all of the compounds from the *X*-O4O-*X* series and all the biphenyl products which were recrystallized from toluene with ethanol. Products were obtained in yields of 40–80%.

1O-5-O1 ^{1}H NMR ($CDCl_3$, δ) 8.4 (s, 2H, $C\underline{H}$=N); 7.8 (d, J = 8.25 Hz, 4H, aromatic); 7.3–7.1 (m, 8H, aromatic); 7.0 (d, J = 8.5 Hz, 4H, aromatic); 3.9 (s, 6H, $OC\underline{H}_3$); 2.6 (t, J = 7.5 Hz, 4H, $ArC\underline{H}_2CH_3$); 1.7 (qn, J = 7.5 Hz, 4H, $CH_2C\underline{H}_2CH_2C\underline{H}_2CH_2$); 1.4 (m, 2H,

$CH_2CH_2C\underline{H}_2CH_2CH_2$). IR (KBr) ν (cm^{-1}): 2912, 2849 (CH_2); 2849 (OCH_3); 3010, 1570 (conjugated C=N); 1606, 1510 (Ar–H); 821 (*p*-substituted aromatic).

2.8. *Thermal characterization*

The thermal behaviour of the dimers was investigated by differential scanning calorimetry using a Mettler Toledo DSC 820 differential scanning calorimeter equipped with a TS0801RO sample robot and calibrated using indium and zinc standards. The heating profile in all cases was heat, cool and reheat at 10°C min^{-1} with a 3 min isotherm between heating and cooling. All samples were heated from 0°C to 20–40° above their clearing temperatures. Thermal data were normally extracted from the second heating trace. Phase characterization was performed using polarizing optical microscopy using an Olympus BH2 polarizing light microscope equipped with a Linkam TMS 92 hot stage.

Results and discussion

3.1. *m-OnO-m and m-n-m series*

Table 1 lists the transitional properties for the *m*-O*n*O-*m* compounds. Nematic phases were assigned from their schlieren optical textures which flashed when subjected to mechanical stress, combined with the high mobility of the phase. 1-O4O-1 and 2-O4O-2 exhibit enantiotropic nematic behaviour, whereas 1-O3O-1 and 2-O3O-2 are not liquid crystalline. The entropy changes associated with the nematic–isotropic transitions are typical for even-membered dimers [12]. A virtual T_{NI} has been estimated for 2-O3O-2 at 94°C which is 106°C lower than that observed for 2-O4O-2; this difference is of a similar magnitude to that found for other dimer series [12] suggesting that the virtual T_{NI} is a realistic value. The melting temperatures are also considerably lower for the odd members than for the corresponding even members. The entropy changes associated with the melting transition, however, are larger for the odd than for the even members. This presumably reflects, at least in part, the greater change in the conformational distribution of the spacer when an odd-membered compound melts directly into the isotropic phase than when an even membered compound melts into the nematic phase.

Table 1. Transition temperatures and associated entropy changes for the *m*-O*n*O-*m* and *m-n-m* series. Results in [] refer to virtual transition temperatures obtained by extrapolation from phase diagrams.

Compound	T_{Cr}/°C	T_{NI}/°C	$\Delta S_{Cr}/R$	$\Delta S_{NI}/R$
1-O3O-1	156	—	15.1	—
1-O4O-1	203	213	8.4	1.64
2-O3O-2	146	[94]	11.7	—
2-O4O-2	188	200	7.0	1.26
1-5-1	103	—	10.1	—
1-6-1	168	187	9.4	1.97
2-5-2	88	[27]	7.5	—
2-6-2	122	173	7.0	1.92

The *m*-O*n*O-*m* compounds are structurally very similar to the extensively investigated α,ω-bis(4-alkylaniline-benzylidene-4′-oxy)alkanes,

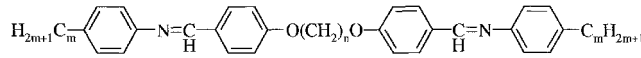

which are referred to using the acronym *m*.O*n*O.*m* [12]. Indeed, the structural difference between the *m*-O*n*O-*m* and *m*.O*n*O.*m* series rests solely with the direction of the Schiff's base linkage; for conventional low molar mass mesogens this has little effect upon transitional behaviour [13]. This appears also to be the case for dimers, as the transitional properties of the *m*.O*n*O.*m* compounds are similar to those of the corresponding members of the *m*-O*n*O-*m* series.

Table 1 also lists the transitional properties of the *m-n-m* series. 1-6-1 and 2-6-2 exhibit enantiotropic nematic behaviour, whereas 1-5-1 and 2-5-2 are not liquid crystalline. A virtual T_{NI} has been estimated for 2-5-2 at 27°C. As with the *m*-O*n*O-*m* compounds, the even members have considerably higher melting points than the odd members, presumably reflecting the difficulty experienced in efficiently packing the bent odd-membered dimers. The entropy changes associated with the melting transitions are now the same, within experimental error, for odd and even members. The nematic–isotropic temperatures of both the odd and even members are lower for the methylene than for the ether-linked dimers and this effect is more pronounced for the odd members. In contrast, $\Delta S_{NI}/R$ is higher for the even methylene-linked dimers than for the corresponding ether-linked dimers. Both these effects are successfully predicted by the theoretical model developed by Luckhurst and co-workers [1].

3.2. *mO-OnO-Om and mO-n-Om series*

In an attempt to enhance the clearing temperatures observed for the *m-n-m* materials we prepared the *m*O-*n*-O*m* series. It is well known that replacing an alkyl terminal chain by an alkyloxy chain typically increases the nematic–isotropic transition temperature of conventional low molar mass materials by 30–40°C [13]. For comparative purposes we also prepared the corresponding ether-linked materials, the *m*O-O*n*O-O*m* compounds.

Table 2 lists the transitional properties of the *m*O-O*n*O-O*m* materials and all four compounds are nematogenic although 1O-O3O-O1 is monotropic. The nematic–isotropic transition temperature of 1O-O4O-O1 is 39°C higher than that of 2-O4O-2 whereas the T_{NI} of

Table 2. Transition temperatures and associated entropy changes for the *m*O-O*n*O-O*m* and *m*O-*n*-O*m* series. Monotropic transition temperatures are given in ( ).

Compound	T_{Cr}/°C	T_{SmN}/°C	T_{NI}/°C	$\Delta S_{CrI}/R$, $\Delta S_{CrN}/R$[a]	$\Delta S_{NI}/R$
1O-O3O-O1	188	—	(175)	17.7	0.28
1O-O4O-O1	212	—	239	8.3[a]	0.97
2O-O3O-O2	177	—	186	16.1[a]	0.39
2O-O4O-O2	210	—	240	10.3[a]	1.15
1O-5-O1	123	(83)	(86)	11.4	—
1O-6-O1	140	—	214	9.9[a]	2.21
2O-5-O2	130	(106)	(107)	10.8	—
2O-6-O2	134	—	223	9.0[a]	2.71

1O-O3O-O1 is 81°C higher than the estimated T_{NI} for 2-O3O-2. Thus, the increase in T_{NI} for the odd member on replacing an ethyl substituent by a methoxy group is similar to that typically observed for conventional low molar mass materials, but for the even member it is somewhat lower than expected. The melting points and nematic–isotropic transition temperatures of the even members are considerably higher than those of the odd members; as we have seen, this is archetypal behaviour of liquid crystal dimers [1, 2]. Similarly, the entropy change associated with the nematic–isotropic transition is larger for the even than for the odd members. By contrast, the entropy changes associated with the melting transition are larger for the odd members than for the even, but again this is typical behaviour although the differences are somewhat larger than seen for the *m*.O*n*O.*m* series [12].

The transitional properties of the *m*O-*n*-O*m* compounds are also listed in table 2. The four compounds exhibit nematic behaviour although the compounds with odd-membered spacers are monotropic in nature. In addition, on cooling the nematic phase of the odd members, the schlieren texture changed to give coexisting regions of focal-conic fan and schlieren textures. A similar texture, but containing somewhat more truncated fans, is exhibited by CN-5-CN, see figure 3. The monotropic nature of the smectic phase precluded its further structural study.

The nematic–isotropic transition temperatures of the *m*O-*n*-O*m* compounds are lower than those of the corresponding *m*O-O*n*O-O*m* materials and this reduction is considerably greater for the odd members. The values of $\Delta S_{NI}/R$ exhibited by the even membered methylene-linked materials are significantly larger than those of the ether-linked compounds. Thus, the transitional properties of these compounds are again in accord with the predictions of Luckhurst and co-workers [1]. It is interesting to note that, as for the *m*-O*n*O-*m* and *m*-*n*-*m* compounds, the entropy change associated with the melting transition is again similar for the corresponding odd- and even-membered dimers. The increase in T_{NI} on passing from 2-5-2 to 1O-5-O1 is 59°C and from 2-6-2 to 1O-6-O1 is 41°C. As before, therefore, the enhancement in T_{NI} on replacing an ethyl group by a methoxy

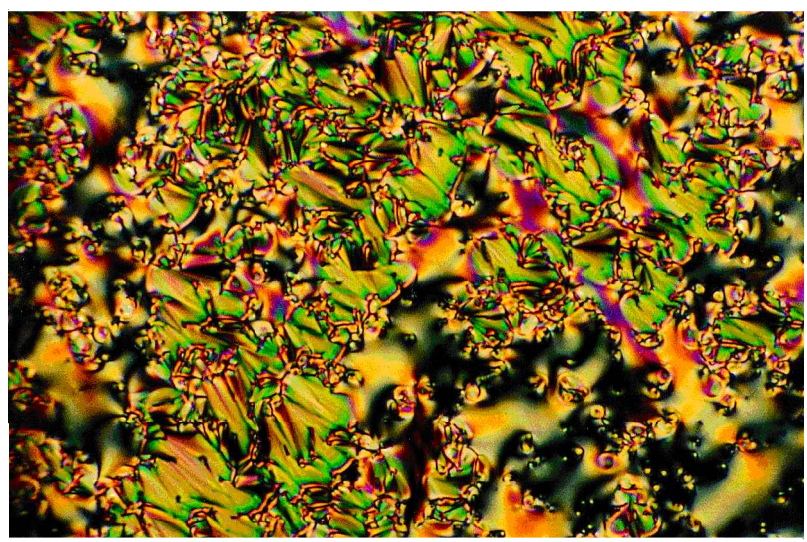

Figure 3. The optical texture exhibited by the smectic phase of CN-5-CN.

substituent is somewhat larger for the odd-membered dimer.

We are now in a position to comment on how the location of the ether oxygen, i.e. either linking the spacer or the terminal chains to the mesogenic units, affects the nematic–isotropic transition temperatures. If we start with 2-6-2 and replace the ethyl chains with methoxy groups, i.e. to obtain 1O-6-O1, then, as we have seen, T_{NI} increases by 41°C, while replacing methylene groups in the spacer giving 2-O4O-2 causes T_{NI} to increase by 27°C. Replacing all four methylene units to give 1O-O4O-O1 enhances T_{NI} by 66°C. Thus, for this system T_{NI} is more sensitive to replacing the outer methylene groups, and the effect of substituting the outer and inner methylene groups is essentially additive. If we now consider an odd-membered system, passing from 2-5-2 to 1O-5-O1 increases T_{NI} by 86°C while going to 2-O3O-2 sees a slightly lower increase of 67°C. At first sight this is a surprising result as it suggests that the outer positions for the ether oxygens have a more important role in determining the average molecular shape. Going from 2-5-2 to 1O-O3O-O1, T_{NI} increases by 148°C and so the effects again appear to be simply additive. The generality of these observations should now be investigated.

The only members of the *m*O-O*n*O-O*m* and *m*O-*n*-O*m* materials to exhibit smectic behaviour are 1O-5-O1 and 2O-5-O2. For the *m*.O*n*O.*m* family of compounds, smectic behaviour is only observed if the length of the terminal chains is greater than half the length of the spacer [12]; a similar relationship has been observed for other symmetric dimers [14]. The behaviour of the *m*O-O*n*O-O*m* series is also in accord with these observations. Thus, the observation of smectic behaviour for 1O-5-O1 and 2O-5-O2 is most surprising and we will return to this later.

3.3. *α,ω-Bis(4′-substituted-benzylidene-4-aminophenoxy)alkanes and α,ω-bis(4′-substituted-benzylidene-4-aminophenyl)alkanes*

Table 3 lists the transitional properties of the NO_2-O*n*O-NO_2 and NO_2-*n*-NO_2 compounds. NO_2-O4O-NO_2 and NO_2-6-NO_2 are enantiotropic nematogens. The T_{NI} for NO_2-O4O-NO_2 is higher than that for NO_2-6-NO_2 while the value of $\Delta S_{NI}/R$ exhibited by NO_2-6-NO_2 is slightly larger than that seen for NO_2-O4O-NO_2. NO_2-O3O-NO_2 is a strongly monotropic nematogen although it was possible to measure a value of $\Delta S_{NI}/R$ of 0.56. NO_2-5-NO_2 did not exhibit liquid crystallinity although its isotropic phase can be supercooled to *c.* 90°C. Thus the reduction in T_{NI} on passing from NO_2-O3O-NO_2 to NO_2-5-NO_2 must be in excess of 50°C, while on going from NO_2-O4O-NO_2 to NO_2-6-NO_2 T_{NI} falls by 19°C. Again the behaviour of these compounds is in accord with the predictions made by Luckhurst and co-workers [1].

CN-O4O-CN and CN-6-CN are enantiotropic nematogens, see table 3. Again, T_{NI} is higher for CN-O4O-CN, while $\Delta S_{NI}/R$ is greater for CN-6-CN. CN-O3O-CN is also an enantiotropic nematogen and $\Delta S_{NI}/R$ is, within experimental error, identical to that exhibited by its biphenyl analogue, i.e. 1,3-bis(4-cyanobiphenyl-4′-oxy)-propane [4]. CN-5-CN exhibits a monotropic nematic phase and the associated clearing entropy is considerably smaller than that observed for CN-O3O-CN. Again, the difference in T_{NI} between the odd members, 83°C, is greater than that between the even members, 12°C.

In addition to a nematic phase, CN-5-CN exhibits a monotropic smectic phase. The optical texture shown by this phase consists of truncated focal-conic fans in coexistence with regions of schlieren-like texture, see figure 3. The monotropic nature of the phase precluded further structural studies.

Table 3. Transition temperatures and associated entropy changes for the *X*-O*n*O-*X* and *X*-*n*-*X* series.

Compound	T_{Cr}/°C	T_{NI}, T_{SmN}[a]/°C	$\Delta S_{Cr}/R$	$\Delta S_{NI}/R$, $\Delta S_{SmN}/R$[a]
NO_2-O3O-NO_2	200	(140)	14.1	0.56
NO_2-O4O-NO_2	191	238	7.4	1.12
NO_2-5-NO_2	130	—	13.5	—
NO_2-6-NO_2	179	219	13.4	1.30
CN-O3O-CN	187	208	11.3	0.57
CN-O4O-CN	225	273	10.5	1.84
CN-5-CN	147	(125), (113)[a]	9.7	0.13, 0.16[a]
CN-6-CN	176	261	8.2	2.43
BP-O3O-BP	243	256	17.2	0.22
BP-O4O-BP	270	> 300 (dec)	14.4	—
BP-5-BP	205	—	9.7	—
BP-6-BP	212	293	9.3	1.91

BP-O4O-BP and BP-6-BP are also enantiotropic nematogens, see table 3, although BP-O4O-BP decomposes at temperatures around T_{NI}. The difference in T_{NI} between BP-O4O-BP and BP-6-BP is *c.* 10°C. BP-O3O-BP also exhibits an enantiotropic nematic phase, while BP-5-BP can be supercooled to 195°C without the observation of liquid crystallinity. Thus, T_{NI} has been reduced by at least 60°C on passing from BP-O3O-BP to BP-5-BP. Again these data are in accord with the predictions made by Luckhurst and co-workers [1].

3.4. *Pyrene-containing dimers*

Table 4 lists the thermal properties of the pyrene-containing dimers (see scheme 3); liquid crystalline behaviour was not observed for any of the four homologues. The melting behaviour of these materials is complex. On first heating, the DSC trace for each compound contains an endotherm associated with the melting transition. On cooling, only Py-6-Py crystallizes, while the other homologues form metastable glassy phases. On reheating, Py-O4O-Py and Py-5-Py exhibit only a glass transition at 174°C and 49°C, respectively. Py-O3O-Py also exhibits a glass transition, at 70°C, but on increasing the temperature further undergoes cold crystallization and at still higher temperatures melts, see figure 4.

The analogous compounds to the Py-O*n*O-Py series have been prepared in which the Schiff's base linkage is reversed [15]. The propyl member of this series also was not liquid crystalline, but showed at T_g at 70°C. Thus, this behaviour is very similar to that observed for Py-O3O-Py. By contrast, the butyl member exhibited a nematic–isotropic transition at 188°C and a T_g at 66°C. For Py-O4O-Py the formation of a glass phase presumably precludes the observation of liquid crystallinity. The glass-forming behaviour of pyrene-containing materials has been attributed to intermolecular face-to-face association of the pyrene moieties. Thus the molecular significance of the large increase in T_g on reversing the Schiff's base link is unclear and requires further study.

Table 4. Transition temperatures and associated entropy changes for the pyrene-substituted dimers.

Compound	T_{Cr}/°C	T_g/°C	$\Delta S_C/R$
Py-O3O-Py	227	70	13.0
Py-O4O-Py	288	174	13.1
Py-5-Py	180	49	9.4
Py-6-Py	178	—	12.9

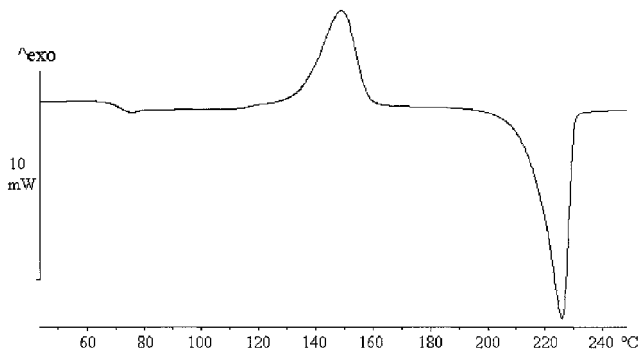

Figure 4. DSC trace obtained on reheating Py-O3O-Py.

3.5. *A comparison of the series*

The efficiency of the terminal group in enhancing the nematic–isotropic transition temperature is essentially the same for both odd- and even-membered ether- and methylene-linked dimers, and in accord with the behaviour of conventional low molar mass mesogens [13]. This similarity has been noted for other series of symmetric liquid crystal dimers [1, 2]. It is difficult to make a similar comparison of the effect of the terminal substituent on the entropy change associated with the nematic–isotropic transitions as the data set is rather incomplete. In general, however, the more the substituent preserves the shape anisotropy of the molecule the higher $\Delta S_{NI}/R$, as would be expected.

Only three compounds prepared in this investigation exhibit smectic behaviour, namely, 1O-5-O1, 2O-5-O2 and CN-5-CN. It is important to note that their ether-linked analogues are exclusively nematic. Given that the principal difference between the ether- and methylene-linked materials lies with their shapes, it appears reasonable to assume that this must be reflected in the structure of the smectic phase. This strongly suggests an alternating smectic C phase as shown in figure 5, and such

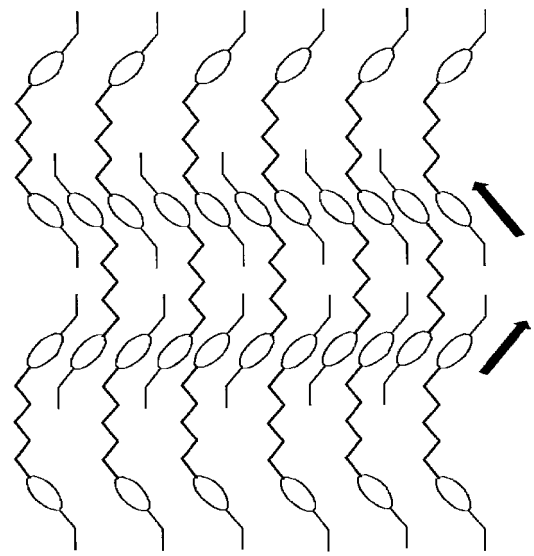

Figure 5. Sketch of an alternating smectic C phase composed of highly bent liquid crystal dimers.

an arrangement is consistent with the observed optical textures. The highly bent pentamethylene-linked dimers can pack efficiently into such a structure while the more linear ether-linked materials cannot. It is interesting to note that the arrangement shown in figure 5 can only accommodate terminal chains which are less than half the spacer length; this is now under investigation.

4. Summary

A range of liquid crystal dimers has been prepared containing either ether-linked or methylene-linked spacers. Changing the spacer from being ether-linked, i.e. $O(CH_2)_nO$, to methylene-linked, i.e. $(CH_2)_{n+2}$, results in decreased nematic–isotropic transition temperatures and this reduction is more pronounced for odd-membered spacers. By contrast, the entropy change associated with the nematic–isotropic transition is higher for an even-membered methylene-linked dimer than for the corresponding ether-linked material. This trend is reversed for odd members. These observations are completely in accord with the predictions of a theoretical model developed by Luckhurst and co-workers [1] in which the only difference between the dimers is their shape. In addition, only highly non-linear pentamethylene-linked dimers exhibited smectic behaviour and it was proposed that an alternating structure was adopted which allows for the efficient packing of the bent molecules. Thus, it would appear that the differences in the transitional properties of ether- and methylene-linked dimers can be accounted for solely in terms of geometrical factors.

References

[1] Imrie, C. T., and Luckhurst, G. R., 1998, *Hand Book of Liquid Crystals*, Vol. 2B, edited by D. Demus, J. W. Goodby, G. W. Gray, H. W. Spiess and V. Vill (Weinheim: Wiley-VCH), Chap. X.

[2] Imrie, C. T., 1999, *Structure and Bonding*, Vol. 95 (Berlin, Heidelberg: Springer Verlag), Chap. 4.

[3] Luckhurst, G. R., 1995, *Macromol. Symp.*, **96,** 1.

[4] Emsley, J. W., Luckhurst, G. R., Shilstone, G. N., and Sage, I., 1984, *Mol. Cryst. liq. Cryst.*, **102,** 223.

[5] Barnes, P. J., Douglass, A. G., Heeks, S. K., and Luckhurst, G. R., 1993, *Liq. Cryst.*, **13,** 603.

[6] Emerson, A. P. J., and Luckhurst, G. R., 1991, *Liq. Cryst.*, **10,** 861.

[7] Ferrarini, A. P. J., and Luckhurst, G. R., 1994, *J. chem. Phys.*, **100,** 1460.

[8] Luckhurst, G. R., 1985, *Recent Advances in Liquid Crystalline Polymers*, edited by L. L. Chapoy (Elsevier), Chap. 7.

[9] Ferrarini, A., Luckhurst, G. R., Nordio, P. L., and Roskilly, S. J., 1993, *Chem. Phys. Lett.*, **214,** 409.

[10] Ferrarini, A., Luckhurst, G. R., Nordio, P. L., and Roskilly, S. J., 1996, *Liq. Cryst.*, **21,** 373.

[11] Keller, P., and Liebert, L., 1978, *Solid State Physics*, Suppl. 14, edited by H. Ehrenreich, F. Seitz, D. Turnbull, and L. Liebert (New York: Academic Press), pp. 25–32.

[12] Date, R. W., Imrie, C. T., Luckhurst, G. R., and Seddon, J. M., 1992, *Liq. Cryst.*, **12,** 203.

[13] Gray, G. W., 1979, in *The Molecular Physics of Liquid Crystals*, edited by G. R. Luckhurst and G. W. Gray (Academic Press), Chap. 1.

[14] Blatch, A. E., and Luckhurst, G. R., 2000, *Liq. Cryst.*, **27,** 775.

[15] Attard, G. S., and Imrie, C. T., 1992, *Liq. Cryst.*, **11,** 785.